Heliyon 7 (2021) e07370

Contents lists available at ScienceDirect

Heliyon

journal homepage: www.cell.com/heliyon

Research article

Novel greenly synthesized titanium dioxide nanoparticles compared to liposomes in drug delivery: in vivo investigation on Ehrlich solid tumor model

Doaa.A. Abdel Fadeel [b,*], Magda.S. Hanafy [a], Nermeen.A. Kelany [a], Mohammed.A. Elywa [a]

[a] Biophysics Branch, Physics Department, Faculty of Science, Zagazig University, 44519 Zagazig, Egypt
[b] Pharmaceutical Technology Unit, Department of Medical Applications of Laser, National Institute of Laser Enhanced Sciences, Cairo University, Cairo, Egypt

ARTICLE INFO

Keywords:
Titanium dioxide nanoparticles
Green synthesis
Liposomes
Drug delivery
Doxorubicin

ABSTRACT

Aims: In a previous work, a pure crystalline titanium dioxide nanoparticles (TiO_2NPs) were synthesized by green synthesis technique using Aloe vera leaves extract as reducing agent. In this work, we are aiming to investigate the potential of the novel greenly synthesized TiO_2NPs as a nano-drug delivery system for the anticancer drug, doxorubicin (Dox).

Main methods: The cytotoxicity of the synthesized TiO_2NPs was tested on two cell lines; normal human skin fibroblasts (HSF) and breast adenocarcinoma cells (MCF-7). Then, Dox was loaded to both TiO_2NPs (Dox- TiO_2NPs) and liposomes (Dox-Lip). The loaded nanoparticles were characterized by TEM, FTIR, encapsulation efficiency, particle size and zeta potential measurement. Moreover, in vitro drug release was studied. Ehrlich tumor-bearing mice were used to study the anticancer activity of Dox- TiO_2NPs, Dox-Lip, and aqueous Dox solution. Tumor volume, survival rate, and histopathological alterations were compared in all groups.

Key findings: Dox was successfully loaded to both liposomes and TiO_2NPs with an encapsulation efficiency of 77% and 65%, respectively. The particle size of Dox-TiO_2NPs, and Dox-Lip was 14.53 nm, and 103 nm, respectively. The cumulative Dox released from TiO_2NPs and liposomes after 4 h was 18 and 46%, respectively.

Dox-Lip and Dox-TiO_2NPs resulted in the highest degree of tumor growth inhibition with 100% and 83% of treated animals remained alive, respectively.

Significance: The greenly synthesized TiO_2NPs were proved to be as effective as liposomes in enhancing the anticancer activity of Dox.

1. Introduction

Nano-based drug delivery has emerged as a potential strategy of anticancer drug targeting to maximize the chemotherapeutic effect and minimize the undesirable effects on healthy tissues [1]. Nano-range size results in a large surface area allowing high efficiency of drug loading. Furthermore, nanoparticles improve drug pharmacokinetics and biodistribution by increasing the ability to append to cell surface markers leading to adequate diffusing into the cells [2].

Recently, titanium dioxide nanoparticles (TiO_2NPs) have a significant consideration in a variety of biomedical applications owing to their appealing photocatalytic properties, high stability, high biocompatibility, and low toxicity [3].

The shape, size, and other properties of TiO_2NPs can be controlled by the method of synthesis [4]. Unfortunately, most of the synthesis pathways require exceedingly costly and dangerous chemicals that cause eco-toxicological problems upon discharge. On the contrary, the green synthesis of TiO_2NPs from plant extracts and other biodegradable materials is considered less poisonous and more eco-accommodating [5]. The green synthesis technique was deployed recently for the synthesis of several types of metal nanoparticles, for example magnetic nanoparticles [6], gold nanoparticles [7], and silver nanoparticles [8]. In addition, TiO_2NPs were greenly synthesized from different plant extracts [9], e.g. leaves extract of Jatropha curcas [5], and root extract of Withania somnifera [10].

* Corresponding author.
E-mail addresses: doaa.fadeel@niles.edu.eg, d_fadeel@yahoo.com (Doaa.A. Abdel Fadeel).

https://doi.org/10.1016/j.heliyon.2021.e07370
Received 29 September 2020; Received in revised form 27 January 2021; Accepted 17 June 2021

Generally, TiO_2NPs are composed of a mixture of crystalline phases as anatase, rutile, and brookite, among them, the anatase phase is the most thermodynamically stable. Therefore, the synthesis of TiO_2NPs with pure anatase crystal phase is a quite challenge [11].

Previously, we succeed to synthesize pure crystalline TiO_2NPs, composed of only anatase phase, by eco-friendly green synthesis technique using Aloe vera leaves extract as a reducing agent at pH 9 [12]. Aloe vera extract was chosen owing to its specific components that are responsible for the metal precursors reduction and hence, nanoparticles formation [9]. The used technique was cost effective, time saving, and ecofriendly that did not use hazardous chemicals. Moreover, the synthesized TiO_2NPs were composed of only pure crystalline anatase phase and exhibited spherical shape with a nano-range particle size (approximately 13 nm).

In this work, we hoped to investigate the anticancer efficacy of this novel greenly synthesized TiO_2NPs and their potential as a drug delivery system of an anti-cancer drug.

TiO_2NPs can adsorb drugs on their surface or encapsulate them inside their reservoir, providing in both cases a sustained controlled drug release. Therefore, they have been used as a drug delivery system for various anticancer drugs, such as daunorubicin [13], cisplatin [14], and doxorubicin [3,15].

Moreover, TiO_2NPs have been used in combination with other nanomaterials as mesoporous zinc oxide [16], and magnetic iron oxide nanoparticles [17] for targeted delivery of curcumin in the treatment of colon cancer.

Doxorubicin (Dox) was selected for this study. Although it is found to have significant cytotoxicity against a wide range of tumor cell lines, the clinical use of Dox is hampered by its serious drawbacks as nephrotoxicity and cardiotoxicity [18]. Besides, tumor cells may develop resistance to Dox due to overexpression of some membrane transporter that actively pumps Dox out of the cells [19,20].

Efforts are continued to design nanotechnology-based carriers that enable Dox to escape the membrane transporters and thus delivering it perfectly to the tumor cells with minimum side effects [21]. Among the nano-formulations that have been studied as Dox carriers, liposomes are the only ones that are approved by the Food and Drug Administration (FDA) in clinical applications, and some liposomal formulation of Dox are commercially available [22,23]. Liposomes are lipid vesicles whose membrane is composed of a phospholipid bilayer with an aqueous core, thus they can incorporate both hydrophilic and hydrophobic drugs [22].

This study may be considered an enhancement of many previous studies that reported the in vitro efficacy of TiO_2NPs a potential nanocarrier for Dox. The novelty of this study relies on the new method of TiO_2NPs synthesis, performing in vivo investigation on tumor-bearing mice, and comparing the efficacy of TiO_2NPs as a Dox nano-carrier to that of liposomes.

2. Materials and methods

2.1. Materials

Titanium tetrachloride ($TiCL_4$), purity≥99%, was purchased from Merck. The plant extract was prepared from healthy leaves of Aloe Vera collected from the botany department, Faculty of Science, Zagazig University, Egypt. Soy Phosphatidylcholine (SPC, from soybean oil), cholesterol 95%, and phosphate-buffered saline (PBS) were purchased from Sigma Aldrich. Ammonium sulfate, chloroform, ethanol, methanol, and other solvents are all of analytical grade were purchased from EL-Nasr pharmaceutical chemicals co. (Adwic, Egypt). Doxorubicin hydrochloride (Adricin®) a product of EIMC united Pharmaceuticals (Badr city, Cairo, Egypt). Ketamine was purchased from Sigma-Tec pharmaceutical company, Egypt. Xylazine was purchased from Adwia pharmaceutical company, Egypt.

Human skin fibroblasts (HSF) and Breast adenocarcinoma (MCF-7) cell lines were obtained from Nawah Scientific Inc., (Mokatam, Cairo, Egypt). Cells were maintained in Dulbecco's Modified Eagle Medium (DMEM media) supplemented with100 mg/mL streptomycin, 100 units/mL penicillin, and 10% heat-inactivated fetal bovine serum (purchased from Lonza, Belgium) in humidified, 5% (v/v) CO_2 atmosphere at 37 °C.

2.2. Synthesis and characterization of TiO_2NP

In previous work, we synthesized titanium dioxide nanoparticles (TiO_2NPs) at room temperature by eco-friendly green synthesis method using Aloe Vera leaves extract at pH 9 [12]. In brief, 100 ml of Aloe vera leaves extract was added dropwise to a 100 ml 1N $TiCL_4$ solution in deionized water under continuous stirring. The pH of the mixture was adjusted at 9 and the stirring is continued at room temperature for 4h. The formed nanoparticles were filtered, washed with double distilled water, and finally dried at 100 °C overnight. The obtained dry powder was further calcined at 500 °C for 4h. The obtained nanoparticles were characterized by x-ray diffraction, FTIR, transmission electron microscopy, and UV-Visible spectrophotometry as early described [12].

2.3. Cytotoxicity of the synthesized TiO_2NPs

The toxicity of the synthesized TiO_2NPs was tested on human skin fibroblasts cell line (HSF) as a model of normal cells, and on breast adenocarcinoma cell line (MCF-7) as a model of cancer cells. Cell viability was assessed by Sulforhodamine-B (SRB) assay. Aliquots of 100 μL cell suspension (5×10^3 cells) were seeded in 96-well plates and incubated in complete media for 24 h. Cells were treated with other aliquots of 100 μL media containing TiO_2NPs at various concentrations (0.01, 0.1, 1, 10 and, 100 μg/ml) and incubated for 72 h. Some cells were incubated for the same period with only fresh media to serve as a control. Afterwards, cells were fixed by replacing media with 150 μL 10% trichloroacetic (TCA) and incubated at 4 °C for 1h. The TCA solution was removed, and the cells were washed with distilled water. Aliquots of 70 μL SRB solution (0.4%w/v) were added and incubated in a dark place at room temperature for 10 min. Plates were washed three times with 1% acetic acid and allowed to be air-dried overnight. Then, 150 μL of 10 mM tris(hydroxymethyl)aminomethane (TRIS) was added to dissolve protein-bound SRB stain; the absorbance was measured at 540 nm using a BMG LABTECH®-FLUO star Omega microplate reader (Ortenberg, Germany). The cell viability of the treated cells was calculated using Eq. (1):

Cell viability (%) of treated cells = Absorbance measured for treated the cells / Absorbance measured for the control untreated cells × 100

Equation (1)

2.4. Loading of the synthesized TiO_2NPs by Dox

Loading of TiO_2NPs by Dox was done as previously described by Chen et al [15]. Briefly, 2 mL aqueous solution of Dox (2 mg/mL) was added to 1 mL aqueous suspension of TiO_2NPs (10 mg/mL) under continuous stirring. The mixture was kept overnight in the dark for the formation of nanocomposite of TiO_2NPs with Dox (Dox-TiO_2NPs) which then lyophilized and stored for further use.

2.5. Preparation of liposomes loaded by Dox

In a clean dry rounded bottom flask, a mixture of SPC and cholesterol (10:1) were completely dissolved in chloroform: methanol mixture (2:1). To form a lipid thin film, the organic solvent was evaporated under vacuum using a rotary evaporator (Heidolph-Elektro GmbH + Co KG, Germany) rotated at a speed of 90 rpm at 50 °C, a temperature above the lipid transition temperature. The film was then hydrated by a 150 mM

aqueous ammonium sulfate solution (pH 5). The formed liposomal vesicles were then centrifuged (KONTRON Centrikon, type 42K, Italy) at 10,000 rpm for 30 min to eliminate the unloaded ammonium sulfate. Dox loading was achieved by remote loading with the ammonium sulfate gradient method [24]. The liposomal suspension was incubated with Dox solution (2 mg/ml) at 60 °C for 2 h. The loaded liposomes were filtered through a microporous filter with a pore size of 450 nm (Whatman nucleopore, Avanti) and kept at 4 °C overnight to allow maturation of the liposomal vesicles loaded by Dox (Dox-Lip).

2.6. Characterization of the prepared nanoparticles and liposomes loaded by Dox

2.6.1. Transmission electron microscopy

The morphology of the TiO_2NPs, Dox-TiO_2NPs, and Dox-Lip was examined by high-resolution transmission electron microscopy (HR-TEM, Tecnai G20, FEI, Nether land). Diluted samples were wetted on a carbon-coated copper grid after negative staining and left to dry before the analysis.

2.6.2. Encapsulation efficiency

The Dox-Lip and Dox-TiO_2NPs suspensions were centrifuged at 10,000 rpm for 30 min at 8 °C (Centrikon T-42 K, Kontron Instruments, UK) to separate the unloaded Dox. The absorbance of Dox in the supernatant was recorded at 480 nm by UV-Visible double beam spectrophotometer (Rayleigh UV-2601). The Dox concentration was calculated from a previously constructed standard calibration curve in distilled water. The encapsulation efficiency (EE) was calculated from Eq. (2) [25]:

Encapsulation efficiency (%) = (Initial amount of drug -Amount of drug in the supernatant /Initial amount of drug) × 100 Equation (2)

2.6.3. Particle size and zeta potential

The average particle size and zeta potential of TiO_2NPs, Dox-TiO_2NPs, and Dox-Lip were measured by dynamic light scattering techniques (Zetasizer, Malvern, UK). The samples were diluted 1:100 by double distilled water and the measurements were done at 25 °C and detection angle 90°.

2.6.4. Fourier transform infrared (FTIR)

FTIR measurements were done to investigate the possible interactions between Dox and TiO_2NPs. FT-IR spectrophotometer (JASCO, FT/IR-4100 type A) was used in the wavenumber range of 400–4000 cm^{-1} to record the functions groups of Dox, TiO_2NPs, and Dox-TiO_2NPs.

2.7. In vitro release of Dox from TiO_2NPs and liposomes

The release of Dox from Dox-Lip and Dox-TiO_2NPs was determined in phosphate-buffered saline (PBS) at pH 7 by the dispersion method [26]. In brief, 2ml of Dox-Lip and Dox-TiO_2NPs suspensions in PBS were centrifuged for 10 min at 10,000 rpm. The liposomal pellets and the precipitated nanoparticles were then dispersed in 1 ml PBS buffer and kept at 37 °C under continuous stirring in a temperature-controlled water bath. At predetermined time intervals, the dispersions were centrifuged and the precipitates were dispersed in a fresh buffer and incubated again, while the amount of the released Dox was determined in the supernatants by UV-Visible spectrophotometer as described above.

2.8. In vivo animal study

2.8.1. Animals and tumor implantation

The animal experimental protocol adhered to ARRIVE guidelines and was carried out after being approved by the Institutional Animal Care and Use Committee, Zagazig University, Egypt (ZU-IACUC), the approval number is ZU-IACUC/1/F/87/2018.

Twenty females, 7-week aged, albino mice of average weight 23 ± 3 g were housed in five clear plastic cages at room temperature (27 ± 3 °C) with a regular light/dark cycle and free access to food and water. The Animals were provided from, and housed in, the animal house of the National cancer institute, Cairo University, Egypt.

After being anesthetized with ketamine/xylazine (100–200 mg/kg) [27], each animal was injected in the thigh of the hind limb with 2×10^6 Ehrlich ascites carcinoma cells in 0.2 ml normal saline (collected from the peritoneal cavity of Ehrlich's ascites carcinoma mice, kindly supplied by the National Institute of Cancer Research, Cairo University).

The treatment protocol began 10 days post tumor implantation when the average tumor volume reached approximately 60 mm^3. The animals were divided randomly into four groups, five animals each, as following: Group1 (control group): received no treatment, Group 2: animals were injected by aqueous Dox solution, Group 3: animals were injected by Dox-TiO_2NPs, Group 4: animals were injected with Dox-Lip. All injections were done intra-tumoral at a dose equivalent to 2.5 mg Dox/kg body weight [28].

The number of mice in each group was calculated statistically according to one way ANOVA design, using Eq. (3) to calculate the minimum and the maximum number of animals in each group (n) [29]:

$$n\ (max) = 20/k + 1,\ n\ (min) = 20/k - 1 \quad \text{Equation (3)}$$

where k is the number of groups

As we have four groups, the maximum number allowed per group is six, and the minimum is four. Consequently, we used five animals in each group.

2.8.2. Assessment of treatment

The tumor length and width were measured weekly using a Vernier caliper for four weeks. The measurements were done at the same particular time of the day each time throughout the experiment. The tumor volume was calculated using Eq. (4) [21]:

$$\text{Tumor volume} = 0.5x\ (d_1)^2\ x\ d_2 \quad \text{Equation (4)}$$

where d_1 and d_2 are the tumor width and length, respectively

The percentage of surviving animals in each group was determined daily and plotted as a function of days post-treatment.

On day 30 post-treatment, the experiment was terminated; and an animal from each group was sacrificed by cervical dislocation. The tumor tissues were excised, fixed in 10% formalin, and embedded in paraffin. Sections were cut at a thickness of 3 μm, stained with hematoxylin and eosin (H&E), and pathologically examined under Olympus BX51 Microscope with Digital Camera to investigate the histopathological changes.

2.9. Statistical analysis

The data were analyzed using SPSS software (SPSS, Inc., Chicago, Illinois, USA). All the results are presented as the mean (of at least three attempts) ± standard deviation. The two-way ANOVA test was used for data analysis followed by post hoc Tukey HSD test of significance, and a *p*-value of less than 0.05 was considered to be statistically significant ($p < 0.05$).

3. Results

3.1. Cytotoxicity of the synthesized TiO_2NPs

The cytotoxicity of the greenly synthesized TiO_2NPs was tested on normal cells (HSF) as well as on cancer cell lines (MCF-7) by SRB assay. In both cell lines, the cell viability did not significantly decrease ($p > 0.05$) at all tested concentrations (0.01–100 μg/ml), as illustrated in Figure 1. At the highest tested concentration (100 μg/ml), the cell viability of HSF, and MCF-7 was 94 ± 0.74%, and 84 ± 0.23%, respectively.

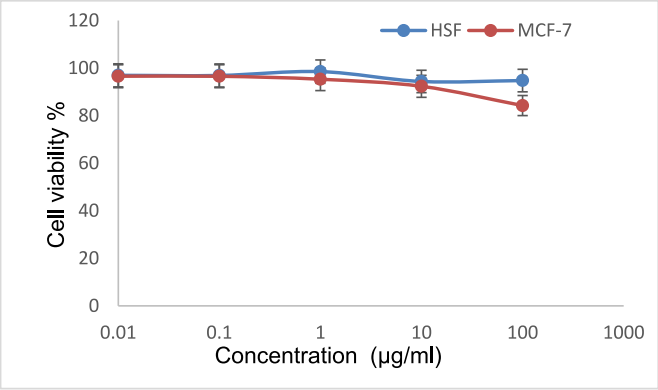

Figure 1. Cell viability of normal human skin fibroblasts (HSF) and breast adenocarcinoma cell line (MCF-7) after treatment by the greenly synthesized TiO_2NPs at different concentrations.

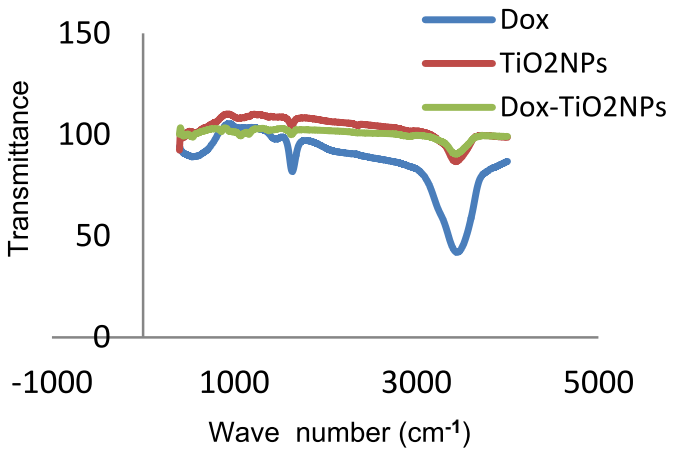

Figure 3. FTIR spectra of aqueous Dox solution, TiO_2NPs and Dox- TiO_2NPs.

3.2. Evaluation of Dox loading to TiO_2NPs

Dox was successfully loaded to TiO_2NPs with an encapsulation efficiency of 65 ± 5%, which is similar to that obtained by Zhang et al [13] who loaded Danurubicin to TiO_2NPs. TEM images of TiO_2NPs and Dox-TiO_2NPs (Figure 2a and b, respectively) showed that both are spherical in shape with a nano-metric size range.

The particle size of TiO_2NPs was 13.3 ± 0.35 nm, which had slightly increased after loading with Dox to 14.53 ± 4.68 nm. Moreover, the synthesized TiO_2NPs showed a zeta potential of (-34.1 ± 5 mV), which was increased to (11.8 ± 5 mV) after Dox loading.

As illustrated in Figure 3, the FTIR spectrum of the TiO_2NPs showed characteristic peaks at 555 cm^{-1} and 1383 cm^{-1} which correspond to the stretching vibration of Ti–O and Ti–O–Ti, respectively. The bands centered at 3435 cm^{-1} correspond to the stretching vibration of hydroxyl groups, while the peak at 1631 cm^{-1} relates to the bending band of adsorbed water molecules on the nanoparticles surface [18]. These results were similar to many previous studies that explained the FTIR spectrum of TiO_2NPs [10,18].

The FTIR spectrum of aqueous Dox solution exhibited characteristic bands at 3447 cm^{-1} attributed to stretching vibration of the hydroxyl group (O–H), peak at 1638 cm^{-1} assigned to (N–H) bending vibration, a peak at 1459 cm^{-1} assigned to C–C stretching vibrations, and peak at 1037cm^{-1} corresponding to C–O stretching vibration. The FRTIR spectrum of Dox-TiO_2NPs showed the characteristic bands of Dox and TiO_2NPs.

3.3. Characterization of the prepared liposomes

Dox was loaded successfully in liposomes with an encapsulation efficiency of (77 ± 5%). TEM photos showed spherical liposomal vesicles with some aggregation (Figure 4). The measured zeta potential was (-36 ± 2.5 mv), indicating good stability of the liposomal vesicles. Dynamic light scattering measurements revealed that Dox loaded liposomes exhibited particle size of 103.8 ± 25 nm.

3.4. In vitro release of Dox from TiO_2NPs and liposomes

The release behavior of Dox from TiO_2NPs and liposomes was investigated at pH 7. The release of Dox from TiO_2NPs and liposomes was sustained for 4 h with the % of cumulative Dox released of 18 and 46%, respectively (Figure 5).

3.5. Evaluation of in vivo antitumor activity

The tumor growth of different groups along four weeks (30 dayes) post-treatment showed significant inhibition in the treated groups compared to the control one ($p < 0.05$) (Figure 6). The tumor volume in Group 3, and Group 4 (received Dox-TiO_2NPs, and Dox-Lip, respectively) was decreased dramatically along the four weeks with no significant difference between them ($p > 0.05$). However, the mean tumor volume of them was significantly lower than ($p < 0.05$) that of Group 2 (received aqueous Dox solution).

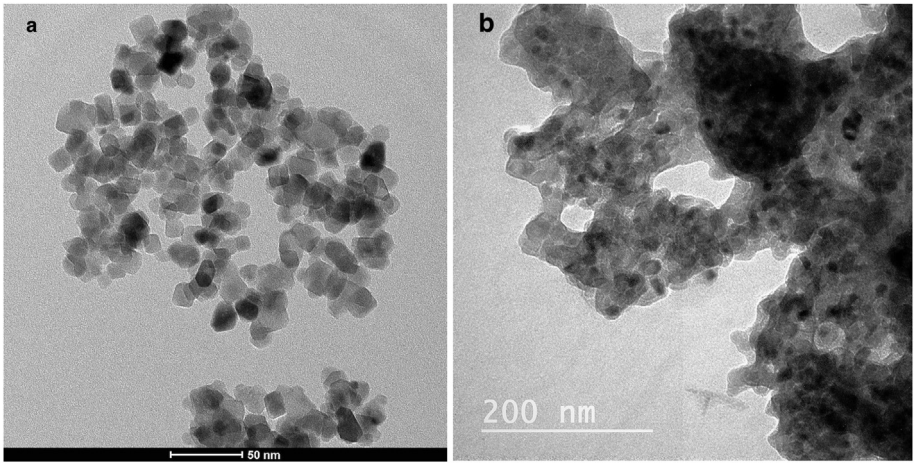

Figure 2. TEM images of: a) TiO_2NPs and b) Dox-TiO_2NPs.

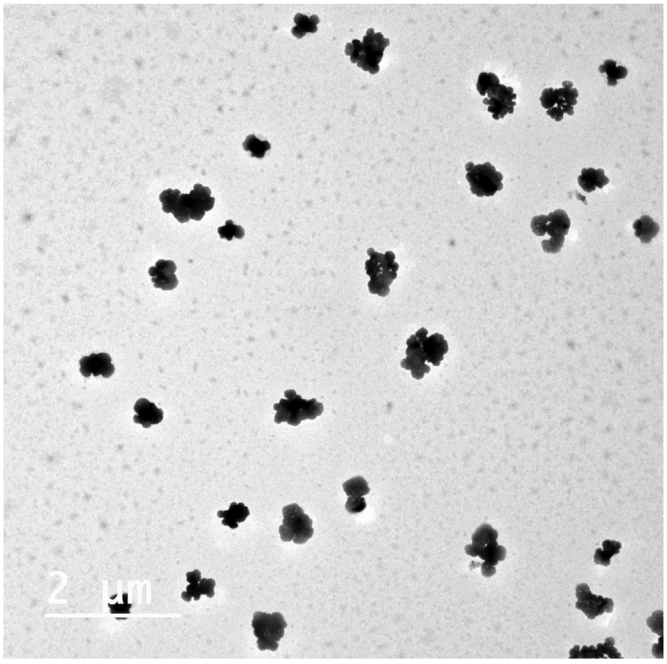

Figure 4. TEM image of Dox-Lip.

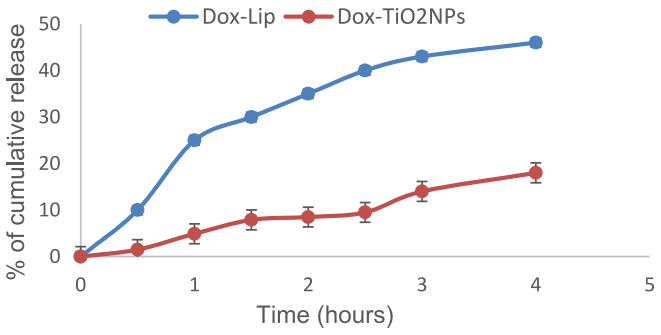

Figure 5. Release profile of Dox from liposomes and TiO_2NPs.

The results of the survival assay revealed that 30 days post-treatment 16.7%, 50%, 83.3%, and 100% of animals in control, aqueous Dox solution, Dox-TiO_2 NPs, and Dox-Lip groups remained alive, respectively (Figure 7). Therefore, animals which received the Dox-lip and Dox-TiO_2 NPs have survived for significantly longer time($p < 0.05$) compared to the other groups. These results were more confirmed by the histopathological examination.

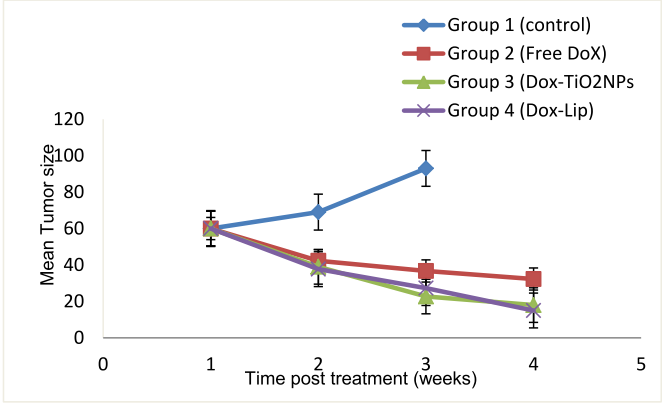

Figure 6. The mean tumor volume for four weeks post treatment in the different animal groups.

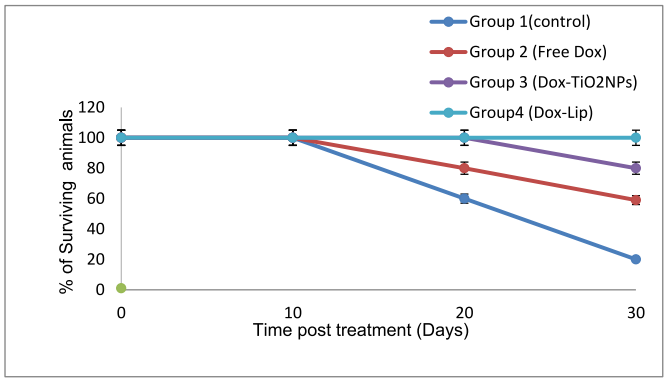

Figure 7. The percentage of surviving animals in different groups along the experiment (for 30 days post treatment).

Tumor sections taken from different groups 30 days post-treatment showed different cellular differentiation of the tumor cells with different areas of necrosis. The sections taken from the control group (Figure 8a) showed undifferentiated epithelioid malignant cells. The sections taken from Group 2 (treated by aqueous Dox solution, Figure 8b) showed wide areas of tumor cells with little necrosis areas (necrosis index was 35%). The sections taken from Group 3 (treated by Dox-TiO_2NPs, Figure 8c) and group 4 (treated by Dox-Lip, Figure 8d), exhibited wide areas of tumor necrosis with minimal scattered degenerated tumor cells (necrosis index was 75% and 85%, respectively). The necrotic tumor appears as structure-less pale eosinophilic debris, devoid of viable nuclei.

4. Discussion

In previous work, we successfully synthesized TiO_2NPs by green synthesis at pH 9 using Aloe Vera leaves extract as a reducing agent. As previously described, the synthesized TiO_2NPs were pure and formed of only the anatase crystalline phase [12]. In this work, we attempted to go deeply into investigating the benefits and the applications of the synthesized TiO_2NPs.

Several previous studies revealed that TiO_2NPs showed prominent cytotoxicity against various carcinoma cell lines, such as human hepatocellular carcinoma cells [30] and human breast cancer cells [31]. Venkatasubbu et al [30] revealed that the TiO_2NPs cytotoxicity was greatly increased upon decreasing the particle size to 3 and 4 nm, at a concentration of 1000 μg/ml. Al-Shabib et al [10] reported that the greenly synthesized TiO_2NPs were non-toxic to normal human embryonic kidney cell line up to 100 μg/ml, however they exhibited dose dependent cytotoxicity to human hepatocellular carcinoma cells. On the contrary, other studies reported that TiO_2NPs showed no cytotoxicity on leukemia cell lines [13]. Therefore, the cytotoxicity of TiO_2NPs may be dependent on many factors as, the synthesis process, the particles size, the concentration used, and the type of the cell line tested.

Our results revealed that the greenly synthesized TiO_2NPs were non-toxic, at concentrations from 0.01 to 100 μg/ml, to normal human skin fibroblast and breast adenocarcinoma cells. Therefore, these nanoparticles can be promising candidates for drug delivery applications; and this pushed us to use them as a nanocarrier for the anticancer drug (Dox).

The synthesized TiO_2NPs were non-covalently loaded by Dox with a relatively high encapsulation efficiency. Qin et al [3] loaded Dox to TiO_2NPs by noncovalent complexation and by covalent conjugation and they revealed that non-covalent complexation was superior because it keeps the main structure of the drug and maximizes its localization in the cells. TEM photos confirmed the spherical structure and nanometric size range of TiO_2NPs before and after Dox loading. This nano-scale size resulted in a tremendous increase in the surface area allowing TiO_2NPs to load high amounts of Dox molecules [23]. Moreover, the small particle size enables the particles to avoid rapid elimination by the reticular

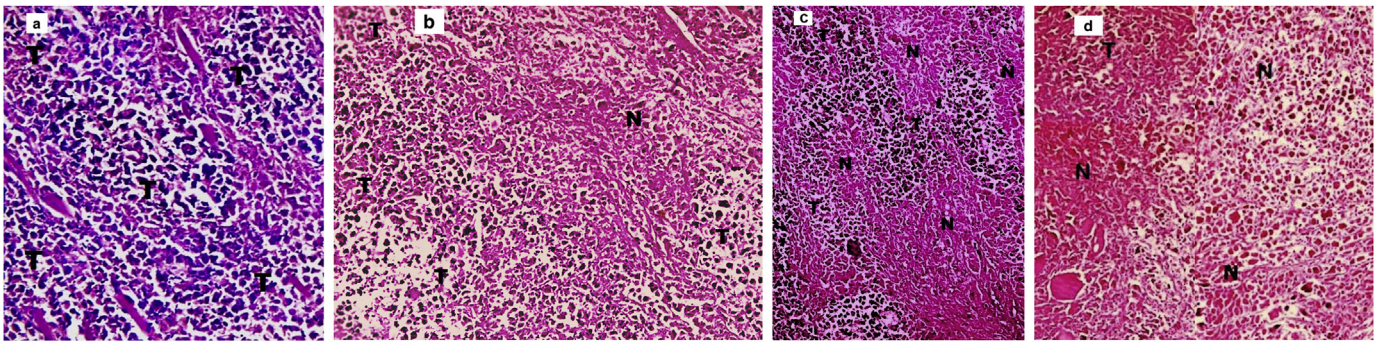

Figure 8. Histopathology images (H&E, X200) of tumor sections taken from: a) control group showing highly malignant undifferentiated tumor cells, b) Dox group showing limited areas of necrosis among the sheets of viable tumor cells, c) Dox-TiO_2NPs group showing wide areas of necrosis, and the residual viable tumor nests, d) Dox-Lip group showing wide areas of necrosis and the residual viable tumor nests. T: tumor cells, N: necrosis.

endothelial system, thus they can passively accumulate in tumor tissues. Passive accumulation took place as a result of the enhanced permeability and retention (EPR) of tumor vasculature which originates as a result of defective vascular endothelial linings and defective lymphatic drainage of growing tumor [13].

Change in the zeta potential can be considered as an indicator of successful Dox loading on the surface of the nanoparticles. Zeta potential measured for the synthesized TiO_2NPs was highly negative, indicating high stability and lack of aggregation. However, the zeta potential was increased to a positive value after Dox loading, which was consistent with previous results obtained by Qin et al [3] and Zhang et al [13]. They explained the complete disappearance of negative charge after Dox loading by the electrostatic interaction between the positively charged Dox molecules and the negatively charged groups of TiO_2NPs, resulting in the self-assembly of Dox molecules on the TiO_2NPs surface [3,13]. Loading of Dox to the synthesized TiO_2NPs was further confirmed by FTIR spectroscopy. The characteristic bands of Dox and TiO_2NPs were kept in the FTIR spectrum of Dox-TiO_2NPs without the formation of new peaks, indicating that physical interaction took place between Dox and the surface of TiO_2NPs [32]. Dox has different reactive functional groups, such as free NH_2, OH, and CO groups [33]. Binding of Dox with nanoparticles surface may be facilitated by the presence of plenty of hydroxyl groups on the TiO_2NPs surface [18].

Being the only FDA approved nano-delivery system for Dox, liposomes loaded by Dox (Dox-Lip) were prepared for comparison.

Despite being hydrophilic, Dox was successfully loaded in liposomes with high encapsulation efficiency. This is attributed to the use of the ammonium sulfate gradient method for Dox loading, in which, a pH gradient was established across the liposomal membrane allowing precipitation of a high amount of the drug in the aqueous core of liposomes [24].

It has been reported that the adequate particle size range is between 10–200 nm since smaller particles are rapidly removed by the kidneys, while larger ones are readily recognized by the reticuloendothelial system [34]. Consequently, both Dox-Lip and Dox-TiO_2NPs have a particle size that is suitable for passive accumulation in tumor tissues by the EPR effect [21,28].

The mechanism of Dox release from nano-delivery systems may be influenced by many factors such as particle size, pH, mode of drug binding, and the surface properties of the nanosystem [35]. The slower release of Dox from TiO_2NPs may be attributed to the strong electrostatic interaction between Dox molecules and TiO_2NPs surface. The sustained release of Dox from liposomes and TiO_2NPs may be beneficial upon intra-tumoral injection, as it provides a high concentration of Dox at the tumor site for a longer time [19].

Although TiO_2NPs have been studied as a potential carrier for Dox by many authors [23,36,37], studies on tumor-bearing animal models are still very limited [38]. Besides, there are many reports about the efficacy of Dox-Lip in enhancing the anticancer effect of Dox [22,28,39], however, there are very few reports about comparing the in vivo antitumor activity of Dox loaded liposomes to Dox loaded in other types of nanoparticles. For example, Mady et al [40] compared the antitumor efficacy of Dox-Lip to that of Dox-Lip loaded in gold nanoparticles in tumor-bearing mice, and revealed that the gold nanoparticles improved the antitumor activity of Dox-Lip.

In this work, the authors tried to elucidate the impact of the novel greenly synthesized TiO_2NPs in enhancing the anticancer activity of Dox in Ehrlich tumor-bearing mice. Furthermore, the anticancer activity of Dox loaded in liposomes and the free aqueous Dox solution were also investigated for comparison. All treated animals were injected intratumorally to permit high distribution inside the tumor tissue, to minimize the systemic toxicity of Dox, and to avoid rapid elimination from the circulation [19]. Collectively, the results of in vivo animal study revealed that the groups treated by Dox-Lip and Dox-TiO_2NPs experienced the highest tumor growth inhibition, the most prolonged survival time as well as the highest necrosis index indicating that the antitumor activity of Dox was significantly improved when loaded in liposomes and greenly synthesized TiO_2NPs. Our results were consistent with those obtained by Du et al [38] who revealed that the Dox loaded on TiO_2NPs was highly effective in inhibiting the tumor growth in the orthotopic breast tumor-bearing mouse model when compared to the free Dox solution. Besides, our results were consistent with those obtained by Elbialy et al [28] who stated that the Dox loaded liposomes caused significant growth inhibition in Ehrlich tumor-bearing mice when compared to the free Dox solution.

The enhancement of the Dox anticancer activity after loading in liposomes and TiO_2NPs may be owing to the passive targeting by the EPR effect and the improvement of cellular uptake by the endocytosis pathway [13,23]. Moreover, Dox was slowly released from liposomes and TiO_2NPs, as described above, allowing the accumulation of Dox in the interstitial tumor tissues for a longer time [28].

5. Conclusion

TiO_2NPs were synthesized by an eco-friendly green synthesis technique using Aloe vera leaves extract as a reducing agent at pH 9. The synthesized TiO_2NPs were pure and composed of only one crystalline phase, which is the thermostable anatase phase. They exhibited spherical shape without aggregation, with nanometric particle size. The synthesized TiO_2NPs were non-toxic for both normal human skin fibroblast and breast adenocarcinoma cells. They were loaded successfully by Dox with high encapsulation efficiency. Dox loading was confirmed by TEM images, FTIR, and change in the zeta potential. Dox was also loaded in liposomes for comparison. Both Dox-loaded TiO_2NPs and Dox-loaded liposomes exhibited spherical shape with nano-range particle size and provided a sustained drug release profile. They have tested for their antitumor activity in Ehrlich tumor-bearing mice and were compared to the free unloaded Dox solution. The results of the in vivo study proved that the greenly synthesized TiO_2NPs could be a promising nano-drug delivery system for Dox, which is as efficient as liposomes. Thus,

greenly synthesized TiO_2NPs could be a promising drug delivery system of Dox in upcoming clinical studies. Further investigation may be required to assess the potential of TiO_2NPs in reducing the undesirable side effect of Dox and other chemotherapeutic drugs.

Declarations

Author contribution statement

Doaa. A. Abdel Fadeel: Performed the experiments; Analyzed and interpreted the data; Contributed reagents, materials, analysis tools or data; Wrote the paper.

Magda. S. Hanafy: Conceived and designed the experiments; Analyzed and interpreted the data; Contributed reagents, materials, analysis tools or data.

Nermeen. A. Kelany; Mohammed. A. Elywa: Performed the experiments; Analyzed and interpreted the data; Contributed reagents, materials, analysis tools or data.

Funding statement

This research did not receive any specific grant from funding agencies in the public, commercial, or not-for-profit sectors.

Data availability statement

Data will be made available on request.

Declaration of interests statement

The authors declare no conflict of interest.

Additional information

No additional information is available for this paper.

References

[1] S. Gurunathan, M.-H. Kang, M. Qasim, J.-H. Kim, Nanoparticle-mediated combination therapy: two-in-one approach for cancer, Int. J. Mol. Sci. 19 (10) (2018) 3264.
[2] N. Bertrand, J.-C. Leroux, The journey of a drug-carrier in the body: an anatomo-physiological perspective, J. Control. release 161 (2) (2012) 152–163.
[3] Y. Qin, et al., Highly water-dispersible TiO2 nanoparticles for doxorubicin delivery: effect of loading mode on therapeutic efficacy, J. Mater. Chem. 21 (44) (2011) 18003–18010.
[4] P. Mathumba, A.T. Kuvarega, L.N. Dlamini, S.P. Malinga, Synthesis and characterisation of titanium dioxide nanoparticles prepared within hyperbranched polyethylenimine polymer template using a modified sol–gel method, Mater. Lett. 195 (2017) 172–177.
[5] S.P. Goutam, G. Saxena, V. Singh, A.K. Yadav, R.N. Bharagava, K.B. Thapa, Green synthesis of TiO2 nanoparticles using leaf extract of Jatropha curcas L. for photocatalytic degradation of tannery wastewater, Chem. Eng. J. 336 (2018) 386–396.
[6] H. Nosrati, M. Salehiabar, E. Attari, S. Davaran, H. Danafar, H.K. Manjili, Green and one-pot surface coating of iron oxide magnetic nanoparticles with natural amino acids and biocompatibility investigation, Appl. Organomet. Chem. 32 (2) (2018), e4069.
[7] S.K. Chinnaiyan, A.M. Soloman, R.K. Perumal, A. Gopinath, M. Balaraman, 5 Fluorouracil-loaded biosynthesised gold nanoparticles for the in vitro treatment of human pancreatic cancer cell, IET Nanobiotechnol. 13 (8) (2019) 824–828.
[8] S. Behboodi, F. Baghbani-Arani, S. Abdalan, S.A.S. Shandiz, Green engineered biomolecule-capped silver nanoparticles fabricated from Cichorium intybus extract: in vitro assessment on apoptosis properties toward human breast cancer (MCF-7) cells, Biol. Trace Elem. Res. 187 (2) (2019) 392–402.
[9] P. Singh, Y.-J. Kim, D. Zhang, D.-C. Yang, Biological synthesis of nanoparticles from plants and microorganisms, Trends Biotechnol. 34 (7) (2016) 588–599.
[10] N.A. Al-Shabib, et al., Phyto-Mediated synthesis of porous titanium dioxide nanoparticles from Withania somnifera root extract: broad-spectrum attenuation of biofilm and cytotoxic properties against HepG2 cell lines, Front. Microbiol. 11 (July) (2020) 1–13.
[11] Z. Fei Yin, L. Wu, H. Gui Yang, Y. Hua Su, Recent progress in biomedical applications of titanium dioxide, Phys. Chem. Chem. Phys. 15 (14) (2013) 4844–4858.
[12] M. Hanafy, D. AbdelFadeel, M. Elywa, N. Kelany, Green synthesis and characterization of TiO 2 nanoparticles using Aloe vera extract at different pH value, Sci. J. King Faisel Univ. 21 (1) (2020) 103–110.
[13] H. Zhang, C. Wang, B. Chen, X. Wang, Daunorubicin-TiO 2 nanocomposites as a 'smart' pH-responsive drug delivery system, Int. J. Nanomed. 7 (2012) 235–242.
[14] E. Liu, et al., Cisplatin loaded hyaluronic acid modified TiO2 nanoparticles for neoadjuvant chemotherapy of ovarian cancer, J. Nanomater. (2015) 2015.
[15] Y. Chen, Y. Wan, Y. Wang, H. Zhang, Z. Jiao, Anticancer efficacy enhancement and attenuation of side effects of doxorubicin with titanium dioxide nanoparticles, Int. J. Nanomed. 6 (2011) 2321–2326.
[16] M. Zamani, M. Rostami, M. Aghajanzadeh, H.K. Manjili, K. Rostamizadeh, H. Danafar, "Mesoporous titanium dioxide@ zinc oxide–graphene oxide nanocarriers for colon-specific drug delivery, J. Mater. Sci. 53 (3) (2018) 1634–1645.
[17] M. Rostami, M. Aghajanzadeh, M. Zamani, H.K. Manjili, H. Danafar, Sono-chemical synthesis and characterization of Fe 3 O 4@ mTiO 2-GO nanocarriers for dual-targeted colon drug delivery, Res. Chem. Intermed. 44 (3) (2018) 1889–1904.
[18] S. Park, et al., Therapeutic use of H2O2-responsive anti-oxidant polymer nanoparticles for doxorubicin-induced cardiomyopathy, Biomaterials 35 (22) (2014) 5944–5953.
[19] H.C. Arora, et al., Nanocarriers enhance doxorubicin uptake in drug-resistant ovarian cancer cells, Canc. Res. 72 (3) (2012) 769–778.
[20] J.-W. Luo, et al., A novel injectable phospholipid gel co-loaded with doxorubicin and bromotetrandrine for resistant breast cancer treatment by intratumoral injection, Colloids Surf. B Biointerfaces 140 (2016) 538–547.
[21] I. Borišev, et al., Nanoformulations of doxorubicin: how far have we come and where do we go from here? Nanotechnology 29 (33) (2018) 332002.
[22] R.S. Fernandes, et al., Doxorubicin-loaded nanocarriers: a comparative study of liposome and nanostructured lipid carrier as alternatives for cancer therapy, Biomed. Pharmacother. 84 (2016) 252–257.
[23] S.A. Shah, M.U.A. Khan, M. Arshad, S.U. Awan, M.U. Hashmi, N. Ahmad, Doxorubicin-loaded photosensitive magnetic liposomes for multi-modal cancer therapy, Colloids Surf. B Biointerfaces 148 (2016) 157–164.
[24] Y. Nie, et al., Cholesterol derivatives based charged liposomes for doxorubicin delivery: preparation, in vitro and in vivo characterization, Theranostics 2 (11) (2012) 1092.
[25] F. Haghiralsadat, et al., New liposomal doxorubicin nanoformulation for osteosarcoma: drug release kinetic study based on thermo and pH sensitivity, Chem. Biol. Drug Des. 90 (3) (2017) 368–379.
[26] D. Abdel Fadeel, G.M. Al-Toukhy, A.M. Elsharif, S.S. Al-Jameel, H.H. Mohamed, T.E. Youssef, Improved photodynamic efficacy of thiophenyl sulfonated zinc phthalocyanine loaded in lipid nano-carriers for hepatocellular carcinoma cancer cells, Photodiagnosis Photodyn. Ther. 23 (2018).
[27] M. Arras, P. Autenried, A. Rettich, D. Spaeni, T. Rülicke, Optimization of intraperitoneal injection anesthesia in mice: drugs, dosages, adverse effects, and anesthesia depth, Comp. Med. 51 (5) (2001) 443–456.
[28] N.S. Elbialy, M.M. Mady, Ehrlich tumor inhibition using doxorubicin containing liposomes, Saudi Pharmaceut. J. 23 (2) (2015) 182–187.
[29] W.N. Arifin, W.M. Zahiruddin, Sample size calculation in animal studies using resource equation approach, Malaysian J. Med. Sci. MJMS 24 (5) (2017) 101.
[30] G.D. Venkatasubbu, S. Ramasamy, G.S. Avadhani, L. Palanikumar, J. Kumar, Size-mediated cytotoxicity of nanocrystalline titanium dioxide, pure and zinc-doped hydroxyapatite nanoparticles in human hepatoma cells, J. Nanoparticle Res. 14 (4) (2012).
[31] K. Murugan, et al., Hydrothermal synthesis of titanium dioxide nanoparticles: mosquitocidal potential and anticancer activity on human breast cancer cells (MCF-7), Parasitol. Res. 115 (3) (2016) 1085–1096.
[32] A. Rudra, R.M. Deepa, M.K. Ghosh, S. Ghosh, B. Mukherjee, Doxorubicin-loaded phosphatidylethanolamine-conjugated nanoliposomes: in vitro characterization and their accumulation in liver, kidneys, and lungs in rats, Int. J. Nanomed. 5 (2010) 811.
[33] S. Liu, A.C.-T. Ko, W. Li, W. Zhong, M. Xing, NIR initiated and pH sensitive single-wall carbon nanotubes for doxorubicin intracellular delivery, J. Mater. Chem. B 2 (9) (2014) 1125–1135.
[34] V. Torchilin, Tumor delivery of macromolecular drugs based on the EPR effect, Adv. Drug Deliv. Rev. 63 (3) (2011) 131–135.
[35] G.D. Venkatasubbu, S. Ramasamy, G.P. Reddy, J. Kumar, In vitro and in vivo anticancer activity of surface modified paclitaxel attached hydroxyapatite and titanium dioxide nanoparticles, Biomed. Microdevices 15 (4) (2013) 711–726.
[36] K.C.-W. Wu, et al., Biocompatible, surface functionalized mesoporous titania nanoparticles for intracellular imaging and anticancer drug delivery, Chem. Commun. 47 (18) (2011) 5232–5234.
[37] W. Ren, et al., Enhanced doxorubicin transport to multidrug resistant breast cancer cells via TiO 2 nanocarriers, RSC Adv. 3 (43) (2013) 20855–20861.
[38] Y. Du, et al., The enhanced chemotherapeutic effects of doxorubicin loaded PEG coated TiO 2 nanocarriers in an orthotopic breast tumor bearing mouse model, J. Mater. Chem. B 3 (8) (2015) 1518–1528.
[39] J. de Oliveira Silva, et al., Folate-coated, long-circulating and pH-sensitive liposomes enhance doxorubicin antitumor effect in a breast cancer animal model, Biomed. Pharmacother. 118 (2019) 109323.
[40] M.M. Mady, F.H. Al-Shaikh, F.F. Al-Farhan, A.A. Aly, M.A. Al-Mohanna, M.M. Ghannam, Enhanced Ehrlich tumor inhibition using DOX-NP^{TM} and gold nanoparticles loaded liposomes, in: AIP Conference Proceedings, 1727, 2016, p. 20014, no. 1.